Nano Energy 63 (2019) 103887

Contents lists available at ScienceDirect

Nano Energy

journal homepage: www.elsevier.com/locate/nanoen

Communication

A facile gaseous sulfur treatment strategy for Li-rich and Ni-rich cathode materials with high cycling and rate performance

Zhenhe Sun[a], Lingqun Xu[a], Caiqiao Dong[a], Hongtao Zhang[a,b], Mingtao Zhang[a], Yanfeng Ma[a,b], Yiyang Liu[c], Zhongjun Li[c], Ying Zhou[a], Yu Han[a], Yongsheng Chen[a,b,*]

[a] The Centre of Nanoscale Science and Technology and Key Laboratory of Functional Polymer Materials, Nankai University, Tianjin, 300071, China
[b] The National Institute for Advanced Materials, Nankai University, Tianjin, 300071, China
[c] College of Chemistry and Molecular Engineering, Zhengzhou University, Zhengzhou, 450001, China

ARTICLE INFO

Keywords:
Cathode materials
Li-rich
Doping
High rate performance
Long cycle life
Gaseous sulfur

ABSTRACT

Lithium-rich and Ni-rich cathode materials have been considered as the attractive candidate for their high capacitive performance, but usually exhibit poor rate performance and limited cycle life. Herein, a facile gaseous sulfur treatment was developed to uniformly create oxygen vacancies and replace oxygen with sulfur atoms at the surface region of lithium-rich and Ni-rich cathode materials. Such a treatment, when applied to typical Li- or Ni- rich materials such as $Li_{1.2}Ni_{0.13}Co_{0.13}Mn_{0.54}O_2$ (LNCMO), $Li_{1.2}Ni_{0.2}Mn_{0.6}O_2$ (LNMO) and $LiNi_{0.8}Co_{0.1}Mn_{0.1}O_2$ (NCM811), could enhance significantly all their cycle and rate performance. For example, LNCMO@S obtained from LNCMO, could exhibit a capacity retention of 81.10% after 600 cycles at 0.5 C (compared with 65.78% of LNCMO after 200 cycles), together with an excellent rate performance of 174.8 mA h g^{-1} at 10 C (compared with 133.3 mA h g^{-1} of LNCMO), which is among the best performance for all Li-rich cathode materials. The revealed mechanism, where the partial replacement of O by S at the lattice surface significantly reduces oxygen partial pressure and also enhances the Li ion conductivity, might shed light on the comprehensive design and control of oxygen activity in transition-metal-oxide systems for Li-ion batteries with high energy and power density.

Lithium-ion batteries (LIBs) have been proved to be one of the most promising energy storage devices to power electric vehicles (EVs) and hybrid electric vehicles (HEVs) due to their high energy density and long cycle life [1,2]. However, the dissatisfactory energy density of LIBs still limits their driving ranges and practical applications [3]. It is generally believed that the capacity of the cathode materials is one of the major limiting factors for the energy density of LIBs [4]. Therefore, Li-rich layered oxide cathode materials (LLOs) and Ni-rich cathode materials have been thought and explored as the possible future choices because of their high specific capacity and low cost [5,6]. However, Li-rich and Ni-rich cathode materials are still facing some fundamental challenges.

LLOs always suffer from the inferior structure instability and voltage decay, which greatly hinder their cycling stability and practical applications [7,8]. The structure instability is closely related to oxygen redox reaction during the activation process of Li_2MnO_3 phase. It has been demonstrated that a reversible oxygen redox reaction occurs in the bulk structure of LLOs, which renders LLOs with extra capacity [9]. However, the surface oxygen atoms are easily oxidized to O_2 and then escape irreversibly from LLOs in the initial cycles [10]. More than that, the escaped oxygen atoms can react with electrolyte easily, resulting in continuous accumulation of non-electroactive species and increased internal impedance [11]. Voltage decay is closely related to the transition metal migration during cycling, which causes the decreasing energy density for Li-ion batteries using these materials. As for Ni-rich cathode materials, the main strategy to increase its discharge capacity is to increase Ni content [12]. However, high Ni content destabilizes the crystal structure and results in oxygen evolution and serious Li/Ni ion mixing placement [13]. Besides, the rate performance of Li- and Ni-rich cathode materials also needs to be improved for realizing commercial application.

Surface coating and bulk doping are common strategies to address these problems of Li-rich and Ni-rich cathode materials [14,15]. Surface coating can physically separate the cathode materials from the electrolyte to avoid the side reactions between them. It can also enhance the electron or ion conductivity depending on coating materials [16,17]. However, surface coating can hardly alter the bulk charging/discharging process, which is closely related to voltage decay for Li-rich

* Corresponding author. The National Institute for Advanced Materials, Nankai University, Tianjin, 300071, China.
E-mail address: yschen99@nankai.edu.cn (Y. Chen).

https://doi.org/10.1016/j.nanoen.2019.103887
Received 13 May 2019; Received in revised form 21 June 2019; Accepted 6 July 2019
Available online 08 July 2019

cathode materials and Li/Ni mixing for Ni-rich cathode materials [18,19]. Doping of foreign ions is a common strategy to stabilize the crystal structure for Li- and Ni-rich cathode materials [19,20]. Cation doping could improve cycle stability of these materials significantly but cation doping sites are difficult to control since several transition metals with different oxidation states coexist in the transition metal layer [21]. Compared with cation doping, anion doping is relatively easy to achieve since there is only one kind of anion O^{2-} in LLOs [21]. Besides, suitable anions give higher reactivity for energy storage and conversion materials [22–24]. Doping of F^{-} anion has been extensively studied since it can stabilize the crystal structure by formation F-M (Ni, Co and Mn) bonds [21,25]. S^{2-} exhibits a lower electronegativity than O^{2-} and the doping of S^{2-} has great potential in enhancing the ionic conductivity of Li- and Ni-rich cathode materials due to their weaker Li–S bonds, [26,27] in addition to the much more convenient handling of solid sulfur. Besides, sulfur doping would inhibit the cation migration between Li and transition metal layers for Li- and Ni-materials due to the larger atom radio of sulfur atom, which is closely related to the voltage decay of Li-rich cathode materials and the Li/Ni mixing of Ni-rich cathode materials [26]. In the rather rare studies for S^{2-} doping, Zhang et al. [27] has explored sulfur atom doping of LLOs by simply mixing Li_2S and LLOs followed by calcining in air and the doped LLOs shows improved but still rather limited rate performance (117 mA h g^{-1} at 5 C).

Recently, Qiu et al. reported that gas-solid interfacial reaction between LLOs and CO_2 could enhance the capacity and rate capability of LLOs largely [28]. Aurbach et al. simply exposed LLOs in NH_3 atmosphere at 400 °C and the obtained cathode material showed enhanced capacity performance and limited average voltage fading [11]. CO_2 and NH_3 can react with oxygen atoms at the surface region of LLOs at suitable temperature [29]. As a result, the oxygen vacancies increase and the oxygen partial pressure goes down at the surface region of LLOs.

Motivated by the considerations above, we proposed a method based on a facile sulfur gas-solid doping treatment of LLOs to reduce oxygen partial pressure at the surface of LLOs. All reactants are solid state at first with a low reaction temperature of 250 °C and there is no further treatment for doping samples, which means that this gaseous sulfur treatment is facile, scalable and environmentally friendly. Such a treatment, when applied to the representative Li- or Ni- rich materials such as $Li_{1.2}Ni_{0.13}Co_{0.13}Mn_{0.54}O_2$ (LNCMO), $Li_{1.2}Ni_{0.2}Mn_{0.6}O_2$ (LNMO) and $LiNi_{0.8}Co_{0.1}Mn_{0.1}O_2$ (NCM811), could all enhance significantly both their cycle and rate performance. For example, the obtained LNCMO@S delivers a reversible capacity of 270.5 mA h g^{-1} (0.05 C, 1 C = 200 mA g^{-1}) with a capacity retention of 81.10% after 600 cycles at 0.5 C (compared with 65.78% of the undoped one LNCMO after 200 cycles), together with an excellent rate performance of 174.8 mA h g^{-1} at 10 C (compared with 133.3 mA h g^{-1} of LNCMO).

The preparation process of LLO@S is shown in Fig. 1. Firstly, solid-state sulfur and LLOs were transferred into the reactor which owned two chambers to hold sulfur and LLOs separately. Next, the reactor was sealed with the assistance of a vacuum pump and alcohol blast burner to avoid sulfur loss and the air interference during the reaction. The sealed reactor was heated to a specific temperature for desired time for the gas-solid reaction. Finally, the LLOs with sulfur doping (LLO@S) was obtained without further purification and no solid sulfur left for all our preparation in the reactor (Fig. S1).

After optimizing the conditions (reaction time, reaction temperature and sulfur content) for the gas-solid reaction, LNCMO@S with an sulfur content of 12 mmol L^{-1} at 250 °C for 8 h shows the best electrochemical performance (Figs. S2 and S3). Optimized LNCMO@S delivers a reversible capacity of 270.5 mA h g^{-1} compared to 261.3 mA h g^{-1} of LNCMO at 0.05 C (Fig. 2a). In the cyclic voltammetry (CV) analysis for LNCMO and LNCMO, the oxidation peaks at around 4.0 and 4.5 V vs Li/Li^+ is associated with oxidation of the Ni–Co–Mn component and activation of the Li_2MnO_3 component, respectively. A new peak emerged at 2.8 V after gaseous sulfur treatment, representing formation of a

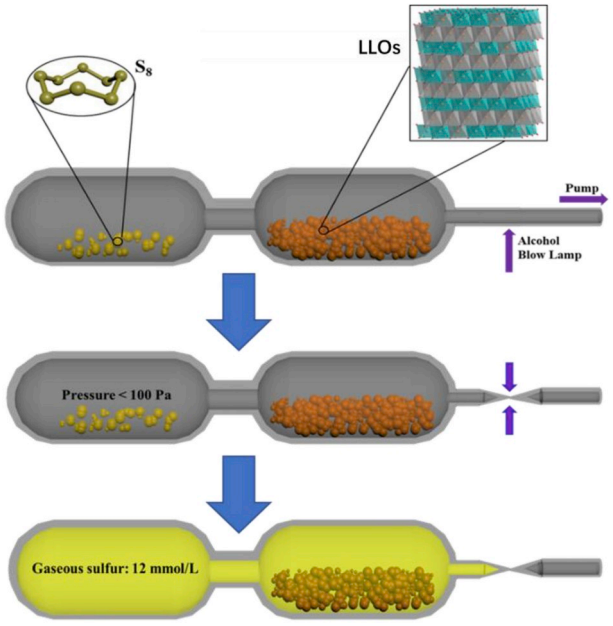

Fig. 1. The schematic diagram of the gaseous sulfur treatment for LLOs.

spinel surface layer induced by the extraction of oxygen and lithium atoms (Fig. S4) [30]. The discharge capacities of LNCMO@S at 0.1, 0.2, 0.5, 1, 2, 5 and 10 C are 268.9, 254.2, 242.3, 233, 221.5, 197.3 and 174.8 mA h g^{-1} (Figs. 2b and S5a), respectively, much higher than the corresponding capacities (254.8, 234.9, 216.3, 199, 184.2, 157.7 and 133.3 mA h g^{-1}) of bare LNCMO at the same rates (Figs. 2b and S5c). As shown in Fig. 2b, when the rate falls back to 0.5 C, LNCMO@S and bare LNCMO recovered their capacity completely, indicating the great structure stability. Fig. 2c, S5b and S5d show the cycle performance for LNCMO@S and bare LNCMO at 0.5 C. After even 600 cycles, LNCMO@S still exhibits a discharge capacity of ~180 mA h g^{-1} with a capacity retention of 81.10%, significantly higher than that of LNCMO (65.78%) after only 200 cycles. Besides, LNCMO@S shows a voltage decay of 0.452 V after 200 cycles, much lower than that of LNCMO (0.674 V) (Fig. S6). LNCMO@S shows a capacity retention of 97.7% and 92.5% at higher current densities (2 C and 5 C) after 100 cycles, respectively, much better than that of LNCMO (78.8% and 75.8%) (Fig. S7). In Fig. S8 and Table S1, we listed and compared the rate and cycle performance of the state of the art LLOs in previous works with this work [16,31–39]. It is clear that the electrochemical performance of LNCMO@S is among the best performance for all Li-rich cathode materials [16,31–39].

Electrochemical impedance spectra (EIS) were measured to explore influence of sulfur doping on the internal impedance and Li ion conductivity of LNCMO@S. Nyquist plots of LNCMO and LNCMO@S electrodes are compared before charging and after 20 and 50 cycles at 0.5 C (Fig. 2d). The plots of LNCMO and LNCMO@S consist of a semicircle in the intermediate-frequency region and a sloped straight line in the low-frequency region. The semicircle in the intermediate-frequency region is correlated with the charge-transfer (R_{ct}) process, and the straight line in the low-frequency region is related to the solid-state diffusion (Warburg impedance, Z_w) of Li ions in the active materials [18,34]. The simulated results and equivalent circuits are shown in Fig. S9. Before cycling, the R_{ct} values of both LNCMO and LNCMO@S electrode are similar and around 115 Ω. After 20 cycles, the R_{ct} Value of both LNCMO and LNCMO@S decreased to a low extent, which could result from the electrochemical activation process [40,41]. The R_{ct} value of LNCMO@S (45.82 Ω) is lower than that of bare LNCMO (77.52 Ω) after 20 cycles and the difference is more obvious at 50th cycle (48.89 and 110.04 Ω for LNCMO@S and bare LNCMO, respectively). This means much more stable surface structure and suppressed

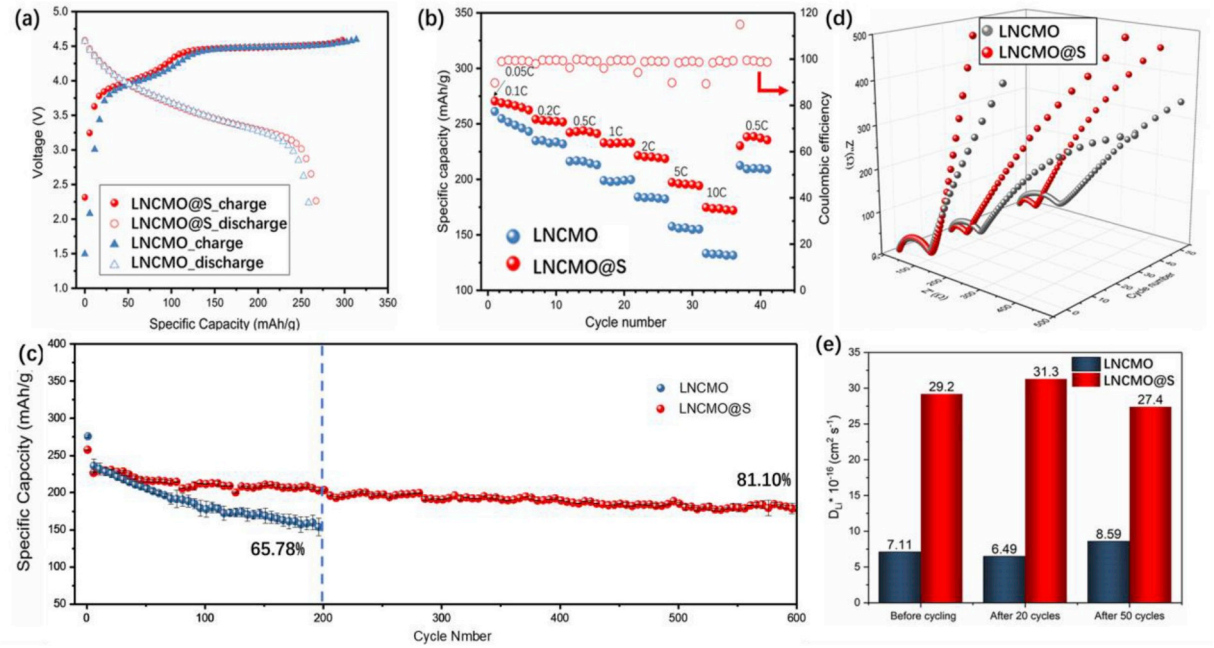

Fig. 2. (a) The initial charge/discharge curve, (b) the high rate and (c) long cycle performance of LNCMO and LNCMO@S based on at least two coin cells. (d) EIS plots and (e) lithium ion diffusion coefficient of LNCMO and LNCMO@S before cycling and after 20 and 50 cycles.

side reactions for LNCMO@S. In addition, the lithium ion diffusion coefficient (D_{Li}) of all samples are calculated from the inclined line in the low-frequency region based on the previous work (Fig. S10) [42]. The results shows that the D_{Li} values of LNCMO@S are 2.74–3.13*10^{-15} $cm^2 s^{-1}$ during cycling, about four times of that of bare LNCMO (6.49–8.59*10^{-16} $cm^2 s^{-1}$) (Fig. 2e). These results agree well with the that of excellent rate performance (Fig. 2b).

To understand the effect of sulfur doping on LNCMO and explore the origin of excellent battery performance, the XRD, XPS, TEM, and EDS characterizations were carried out. The TEM images shows crystallite size is about 50–80 nm and the (003) lattice plane space is about 0.47 nm accorded with the previous work (Fig. S11) [43]. The results of EDS mapping shows that the sulfur distribute uniformly at the surface of LNCMO@S (Fig. S12).The XRD results shown in Fig. 3a indicate that both LNCMO@S and the reference bare LNCMO exhibit the same diffraction peaks and patterns in agreement with literatures, [43,44] indicating that the main crystal structure after sulfur modification remains unchanged. The unit cell parameters (*a* and *c*) of LNCMO@S slightly increases compared to that of bare LNCMO (Fig. 3a and b and S13) and the oxygen occupation decreases to a lower extent after sulfur

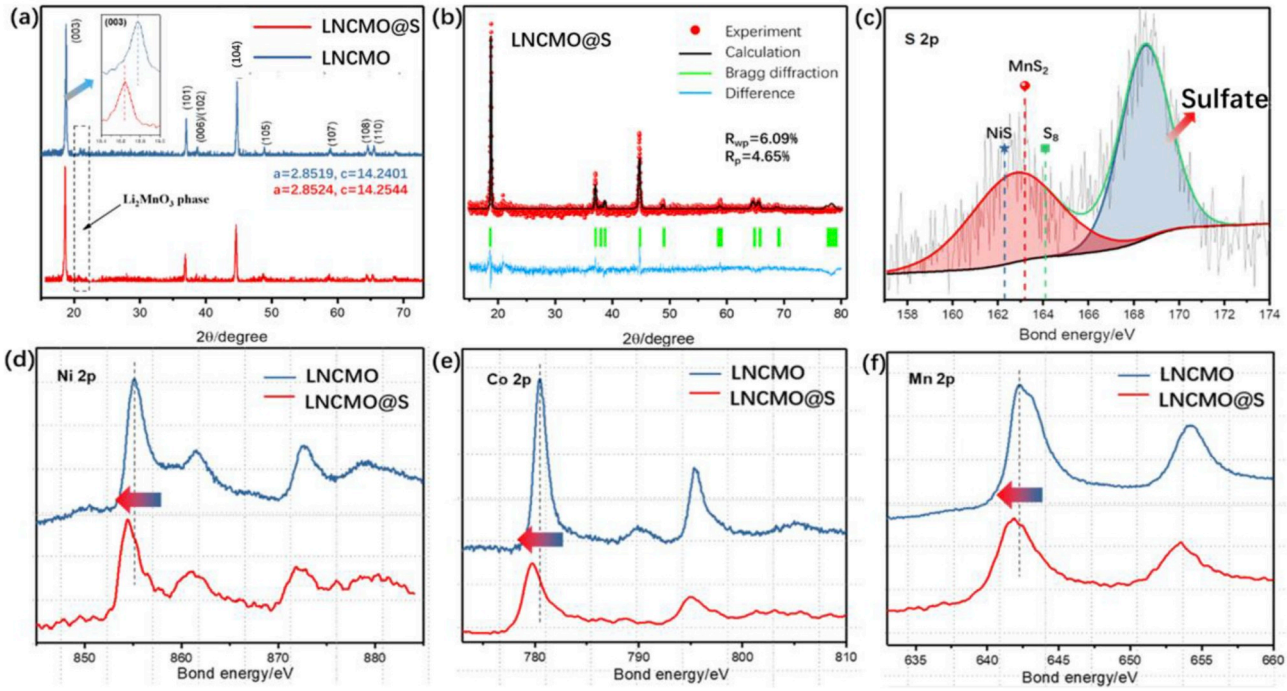

Fig. 3. (a) XRD patterns of $Li_{1.2}Ni_{0.13}Co_{0.13}Mn_{0.54}O_2$ with and without sulfur and (b) the refinement results of LNCMO@S. XPS spectrums of (c) S 2p, (d) Ni 2p, (e) Co 2p, (f) Mn 2p.

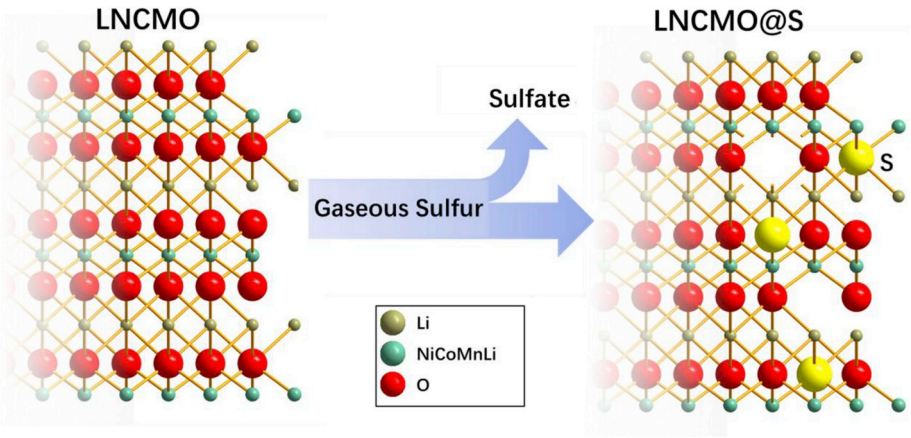

Fig. 4. The partial O replacement doped by S in the lattice of LNCMO.

doping (Table S2).

The XPS measurements were conducted for both LNCMO@S and bare LNCMO to study the variation of bond energy after sulfur doping (Fig. 3c–f). In the XPS spectrum of S 2p (Fig. 3c), the peaks in 160–164 eV region are contributed to the S-Metal bonds [45,46,47] and the peaks in the higher bond energy region (166–171 eV) are ascribed to the S–O bonds from sulfate species, indicating clearly partial replacement of O by S atoms [47,48]. For the XPS data related to the metal ions, LNCMO@S shifts to lower bond energy region (854.3, 779.7, and 641.8 eV for Ni $2p_{3/2}$, Co $2p_{3/2}$ and Mn $2p_{3/2}$, respectively) compared with that (855.1, 780.5 and 642.3 eV, respectively) for the reference bare LNCMO, supporting the partial replacement of O by S. The sulfur content in LNCMO@S is estimated at ~0.77 at% based on the XPS results.

Based on the results of XRD (Fig. 3a and b) and XPS (Fig. 3c–f), it can be concluded that gaseous sulfur reacted with LNCMO at its surface and underwent a disproportionate reaction (Fig. 4). Part of sulfur atoms were reduced and occupied the oxygen sites, inducing the increment of unit cell parameters (Fig. 3a) [49]. The rest reacted with the oxygen and lithium atoms extracted from LNCMO, forming sulfate species in-situ accompanied by the appearance of oxygen vacancies at the surface region. These results agree well with the reduction of oxygen occupation after sulfur doping (Table S2).

The enhanced cycle performance is contributed to the suppressed oxygen evolution and transition metal migration after gaseous sulfur treatment, supported by the much lower voltage decay after gaseous sulfur treatment (Fig. S6) [50,51]. The excellent rate performance would result from the S replacement of O atoms at the surface region of LLOs. It is well known that LLOs own well layered structure with both lithium layer and transition metal layer [34,52] and both transition metal and lithium ions occupy the octahedral sites consisted of oxygen atoms (Fig. 5a). In lithium layers, lithium ions hop between octahedral sites and tetrahedral sites to realize the Li migration (Fig. 5b) [53]. When some oxygen atoms are replaced with the sulfur atoms, it is expected that the migration energy barrier of lithium ions would decrease due to the weaker Li–S bonds. To verify this point, the first-principles calculations were carried out to compare the energy of the migration path (Fig. 5b) of LLO and LLO@S. It is shown that the migration energy barriers of Li ions in the LLO@S (0.53 eV) is much lower than that of LLO (0.71 eV) in Fig. 5c. These results agree well with that of the battery test (Fig. 2b) and EIS (Fig. 2e).

At last, the facile gaseous sulfur treatment is extended to other representative Li-rich and Ni-rich materials such as $Li_{1.2}Ni_{0.2}Mn_{0.6}O_2$ (LNMO) and $LiNi_{0.8}Co_{0.1}Mn_{0.1}O_2$ (NCM811). As shown in Figs. S12 and S13, the obtained LNMO@S retains a discharge capacity of 215 mA h g^{-1} after 150 cycles at 0.5 C with an excellent capacity retention of 98.2% (Fig. S12a). In contrast, bare LNMO only has a discharge capacity of 192.5 mA h g^{-1} with a capacity retention of 94.6% after 150 cycles (Figs. S14a and S15). In addition, the rate performance of LNMO@S is also significantly better than that of LNMO, with the reversible capacity of 196.6 mA h g^{-1} compared with 177.9 mA h g^{-1} at 2 C (Fig. S14b). Similarly, both the cycling and rate performance of NCM811 were improved after gaseous sulfur treatment as shown in Figure S14c, S14d and S14e. The structure of NCM811 and NCM811@S is studied by XRD and there is no clear difference between them, meaning the unchanged structure after sulfur treatment (Fig. S16). The enhanced electrochemical performance of NCM811@S is contributed to the suppressed Li/Ni mixing during cycling caused by the doped sulfur

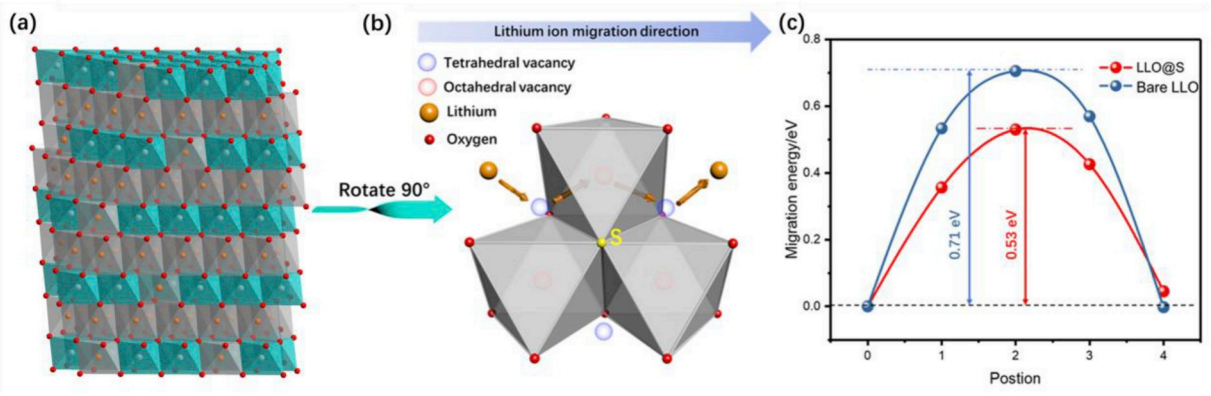

Fig. 5. (a) The layered structure of LLOs. (b) The schematic diagram of lithium ion migration path in the lattice of LLOs and (c) The migration energy barrier from the octahedral site to another one based on the first principle calculations.

atoms [26,54]. These results indicate that the facile gaseous sulfur strategy might be a general approach to realize the sulfur doping and/or enhance the ion conductivity for other transition oxides materials, such as Na ion batteries cathode materials Na_xMO_2 (M = Ni, Co, Mn and so on) [55] and solid-state electrolyte $Li_7La_3Zr_2O_{12}$ [56].

In summary, a facile gaseous sulfur strategy is demonstrated to address the challenging limited rate and cycling issues of Li- and Ni-rich cathode materials caused mainly by oxygen evolution. When applied for the most representative such materials, their rate and cycling performance are all significantly improved. The obtained LNCMO@S shows a high rate performance of 174.8 mA h g^{-1} at 10 C and an excellent capacity retention of 81.10% after 600 cycles at 0.5 C. The revealed mechanism, where the partial replacement of O by S at the lattice surface significantly inhibit oxygen evolution and enhance the Li ion conductivity, is expected to be applied for other cathode materials and solid state electrolyte due to the facile, scalable and inexpensive approach to achieve high energy and power density.

Conflicts of interest

There are no conflicts to declare.

Acknowledgements

Dedicated to the 100th anniversary of Nankai University. The authors gratefully acknowledge the financial support from Ministry of Science and Technology of China (MoST, 2016YFA0200200), the National Natural Science Foundation of China (NSFC, 21421001 and 51633002), Tianjin city (16ZXCLGX00100) and 111 Project (B12015).

Appendix A. Supplementary data

Supplementary data to this article can be found online at https://doi.org/10.1016/j.nanoen.2019.103887.

References

[1] J. Lee, D.A. Kitchaev, D.H. Kwon, C.W. Lee, J.K. Papp, Y.S. Liu, Z. Lun, R.J. Clement, T. Shi, B.D. McCloskey, J. Guo, M. Balasubramanian, G. Ceder, Reversible Mn(2+)/Mn(4+) double redox in lithium-excess cathode materials, Nature 556 (2018) 185–190.
[2] Y. Pei, Q. Chen, Y.-C. Xiao, L. Liu, C.-Y. Xu, L. Zhen, G. Henkelman, G. Cao, Understanding the phase transitions in spinel-layered-rock salt system: criterion for the rational design of LLO/spinel nanocomposites, Nano Energy 40 (2017) 566–575.
[3] Y. Zuo, B. Li, N. Jiang, W. Chu, H. Zhang, R. Zou, D. Xia, A high-capacity O2-type Li-rich cathode material with a single-layer Li2MnO3 superstructure, Adv. Mater. 30 (2018) 1707255.
[4] R.A. House, L. Jin, U. Maitra, K. Tsuruta, J.W. Somerville, D.P. Förstermann, F. Massel, L. Duda, M.R. Roberts, P.G. Bruce, Lithium manganese oxyfluoride as a new cathode material exhibiting oxygen redox, Energy Environ. Sci. 11 (2018) 926–932.
[5] R. Yu, X. Zhang, T. Liu, L. Yang, L. Liu, Y. Wang, X. Wang, H. Shu, X. Yang, Spinel/layered heterostructured lithium-rich oxide nanowires as cathode material for high-energy lithium-ion batteries, ACS Appl. Mater. Interfaces 9 (2017) 41210–41223.
[6] R. Yu, X. Wang, D. Wang, L. Ge, H. Shu, X. Yang, Self-assembly synthesis and electrochemical performance of $Li_{1.5}Mn_{0.75}Ni_{0.15}Co_{0.10}O_{2+\delta}$ microspheres with multilayer shells, J. Mater. Chem. A 3 (2015) 3120–3129.
[7] F. Fu, Y. Yao, H. Wang, G.-L. Xu, K. Amine, S.-G. Sun, M. Shao, Structure dependent electrochemical performance of Li-rich layered oxides in lithium-ion batteries, Nano Energy 35 (2017) 370–378.
[8] S. Liu, Z. Liu, X. Shen, W. Li, Y. Gao, M.N. Banis, M. Li, K. Chen, L. Zhu, R. Yu, Z. Wang, X. Sun, G. Lu, Q. Kong, X. Bai, L. Chen, Surface doping to enhance structural integrity and performance of Li-rich layered oxide, Adv. Energy Mater. 8 (2018) 1802105.
[9] X.-D. Zhang, J.-L. Shi, J.-Y. Liang, Y.-X. Yin, J.-N. Zhang, X.-Q. Yu, Y.-G. Guo, Suppressing surface lattice oxygen release of Li-rich cathode materials via heterostructured spinel Li4Mn5O12 coating, Adv. Mater. 30 (2018).
[10] Y. Shin, K.A. Persson, Surface morphology and surface stability against oxygen loss of the lithium-excess Li2MnO3 cathode material as a function of lithium concentration, ACS Appl. Mater. Interfaces 8 (2016) 25595–25602.
[11] E.M. Erickson, H. Sclar, F. Schipper, J. Liu, R. Tian, C. Ghanty, L. Burstein, N. Leifer, J. Grinblat, M. Talianker, J.-Y. Shin, J.K. Lampert, B. Markovsky, A.I. Frenkel, D. Aurbach, High-temperature treatment of Li-rich cathode materials with ammonia: improved capacity and mean voltage stability during cycling, Adv. Energy Mater. 7 (2017).
[12] D.-S. Ko, J.-H. Park, S. Park, Y.N. Ham, S.J. Ahn, J.-H. Park, H.N. Han, E. Lee, W.S. Jeon, C. Jung, Microstructural visualization of compositional changes induced by transition metal dissolution in Ni-rich layered cathode materials by high-resolution particle analysis, Nano Energy 56 (2019) 434–442.
[13] H.-H. Ryu, K.-J. Park, C.S. Yoon, Y.-K. Sun, Capacity fading of Ni-rich Li [NixCoyMn1−x−y]O2 (0.6 ≤ x ≤ 0.95) cathodes for high-energy-density lithium-ion batteries: bulk or surface degradation? Chem. Mater. (2018), https://doi.org/10.1021/acs.chemmater.7b05269.
[14] B. Han, B. Key, S.H. Lapidus, J.C. Garcia, H. Iddir, J.T. Vaughey, F. Dogan, From coating to dopant: how the transition metal composition affects alumina coatings on Ni-rich cathodes, ACS Appl. Mater. Interfaces 9 (2017) 41291–41302.
[15] H.Z. Zhang, Q.Q. Qiao, G.R. Li, X.P. Gao, PO43− polyanion-doping for stabilizing Li-rich layered oxides as cathode materials for advanced lithium-ion batteries, J. Mater. Chem. 2 (2014) 7454–7460.
[16] Q. Xia, X. Zhao, M. Xu, Z. Ding, J. Liu, L. Chen, D.G. Ivey, W. Wei, A Li-rich Layered@Spinel@Carbon heterostructured cathode material for high capacity and high rate lithium-ion batteries fabricated via an in situ synchronous carbonization-reduction method, J. Mater. Chem. A 3 (2015) 3995–4003.
[17] D. Wang, X. Wang, X. Yang, R. Yu, L. Ge, H. Shu, Polyaniline modification and performance enhancement of lithium-rich cathode material based on layered-spinel hybrid structure, J. Power Sources 293 (2015) 89–94.
[18] P.K. Nayak, J. Grinblat, M. Levi, E. Levi, S. Kim, J.W. Choi, D. Aurbach, Al, Doping for mitigating the capacity fading and voltage decay of layered Li and Mn-rich cathodes for Li-ion batteries, Adv. Energy Mater. 6 (2016).
[19] Z. Sun, L. Xu, C. Dong, H. Zhang, M. Zhang, Y. Liu, Y. Zhou, Y. Han, Y. Chen, Enhanced cycling stability of boron-doped lithium-rich layered oxide cathode materials by suppressing transition metal migration, J. Mater. Chem. A (2019), https://doi.org/10.1039/C8TA10786F.
[20] Q. Li, G.S. Li, C.C. Fu, D. Luo, J.M. Fan, L.P. Li, K+-Doped $Li_{1.2}Mn_{0.54}Co_{0.13}Ni_{0.13}O_2$: a novel cathode material with an enhanced cycling stability for lithium-ion batteries, ACS Appl. Mater. Interfaces 6 (2014) 10330–10341.
[21] L. Li, B.H. Song, Y.L. Chang, H. Xia, J.R. Yang, K.S. Lee, L. Lu, Retarded phase transition by fluorine doping in Li-rich layered $Li_{1.2}Mn_{0.54}Ni_{0.13}Co_{0.13}O_2$ cathode material, J. Power Sources 283 (2015) 162–170.
[22] B.-Q. Li, S.-Y. Zhang, C. Tang, X. Cui, Q. Zhang, Anionic regulated NiFe (Oxy) Sulfide electrocatalysts for water oxidation, Small 13 (2017) 1700610.
[23] H.-F. Wang, C. Tang, B. Wang, B.-Q. Li, Q. Zhang, Bifunctional transition metal hydroxysulfides: room-temperature sulfurization and their applications in Zn–air batteries, Adv. Mater. 29 (2017) 1702327.
[24] D. Liu, X. Fan, Z. Li, T. Liu, M. Sun, C. Qian, M. Ling, Y. Liu, C. Liang, A cation/anion co-doped Li1.12Na0.08Ni0.2Mn0.6O1.95F0.05 cathode for lithium ion batteries, Nano Energy 58 (2019) 786–796.
[25] J. Zheng, X. Wu, Y. Yang, Improved electrochemical performance of Li Li0.2Mn0.54Ni0.13Co0.13 O-2 cathode material by fluorine incorporation, Electrochim. Acta 105 (2013) 200–208.
[26] F. Kong, C. Liang, R.C. Longo, D.-H. Yeon, Y. Zheng, J.-H. Park, S.-G. Doo, K. Cho, Conflicting roles of anion doping on the electrochemical performance of Li-ion battery cathode materials, Chem. Mater. 28 (2016) 6942–6952.
[27] J. An, L. Shi, G. Chen, M. Li, H. Liu, S. Yuan, S. Chen, D. Zhang, Insights into the stable layered structure of a Li-rich cathode material for lithium-ion batteries, J. Mater. Chem. A (2017), https://doi.org/10.1039/c7ta05971j.
[28] B. Qiu, M.H. Zhang, L.J. Wu, J. Wang, Y.G. Xia, D.N. Qian, H.D. Liu, S. Hy, Y. Chen, K. An, Y.M. Zhu, Z.P. Liu, Y.S. Meng, Gas-solid interfacial modification of oxygen activity in layered oxide cathodes for lithium-ion batteries, Nat. Commun. 7 (2016) 10.
[29] H.Z. Zhang, Q.Q. Qiao, G.R. Li, S.H. Ye, X.P. Gao, Surface nitridation of Li-rich layered $Li(Li_{0.17}Ni_{0.25}Mn_{0.58})O_2$ oxide as cathode material for lithium-ion battery, J. Mater. Chem. 22 (2012) 13104–13109.
[30] J.M. Zheng, S.J. Myeong, W.R. Cho, P.F. Yan, J. Xiao, C.M. Wang, J. Cho, J.G. Zhang, Li- and Mn-rich cathode materials: challenges to commercialization, Adv. Energy Mater. 7 (2017) 25.
[31] F. Fu, Q. Wang, Y.-P. Deng, C.-H. Shen, X.-X. Peng, L. Huang, S.-G. Sun, Effect of synthetic routes on the rate performance of Li-rich layered $Li_{1.2}Mn_{0.56}Ni_{0.12}Co_{0.12}O_2$, J. Mater. Chem. A 3 (2015) 5197–5203.
[32] X. Bian, Q. Fu, H. Qiu, F. Du, Y. Gao, L. Zhang, B. Zou, G. Chen, Y. Wei, High-performance $Li(Li_{0.18}Ni_{0.15}Co_{0.15}Mn_{0.52})O_2@Li_4M_5O_{12}$ heterostructured cathode material coated with a lithium borate oxide glass layer, Chem. Mater. 27 (2015) 5745–5754.
[33] R. Yu, X. Wang, Y. Fu, L. Wang, S. Cai, M. Liu, B. Lu, G. Wang, D. Wang, Q. Ren, X. Yang, Effect of magnesium doping on properties of lithium-rich layered oxide cathodes based on a one-step co-precipitation strategy, J. Mater. Chem. A 4 (2016) 4941–4951.
[34] S. Shi, T. Wang, M. Cao, J. Wang, M. Zhao, G. Yang, Rapid self-assembly spherical $Li_{1.2}Mn_{0.56}Ni_{0.16}Co_{0.08}O_2$ with improved performances by microwave hydrothermal method as cathode for lithium-ion batteries, ACS Appl. Mater. Interfaces 8 (2016) 11476–11487.
[35] X. He, J. Wang, R. Wang, B. Qiu, H. Frielinghaus, P. Niehoff, H. Liu, M.C. Stan, E. Paillard, M. Winter, J. Li, A 3D porous Li-rich cathode material with an in situ modified surface for high performance lithium ion batteries with reduced voltage decay, J. Mater. Chem. A 4 (2016) 7230–7237.
[36] A. Bhaskar, S. Krueger, V. Siozios, J. Li, S. Nowak, M. Winter, Synthesis and characterization of high-energy, high-power spinel-layered composite cathode materials for lithium-ion batteries, Adv. Energy Mater. 5 (2015).
[37] P. Oh, M. Ko, S. Myeong, Y. Kim, J. Cho, A novel surface treatment method and new

insight into discharge voltage deterioration for high-performance 0.4Li(2)MnO(3-)0.6LiNi(1/3)Co(1/3)Mn(1/3)O(2) cathode materials, Adv. Energy Mater. 4 (2014).
[38] B. Wu, X. Yang, X. Jiang, Y. Zhang, H. Shu, P. Gao, L. Liu, X. Wang, Synchronous tailoring surface structure and chemical composition of Li-Rich-Layered oxide for high-energy lithium-ion batteries, Adv. Funct. Mater. 28 (2018) 1803392.
[39] J.L. Shi, D.D. Xiao, M. Ge, X. Yu, Y. Chu, X. Huang, X.D. Zhang, Y.X. Yin, X.Q. Yang, Y.G. Guo, L. Gu, L.J. Wan, High-capacity cathode material with high voltage for Li-ion batteries, Adv. Mater. (2018), https://doi.org/10.1002/adma.201705575.
[40] G.R. Li, X. Feng, Y. Ding, S.H. Ye, X.P. Gao, AlF3-coated Li($Li_{0.17}Ni_{0.25}Mn_{0.58}$)$O_2$ as cathode material for Li-ion batteries, Electrochim. Acta 78 (2012) 308–315.
[41] H. Zhang, T. Yang, Y. Han, D. Song, X. Shi, L. Zhang, L. Bie, Enhanced electrochemical performance of Li(1.2)Ni(0.13)CO(0.13)Mr(0.54)O(2) by surface modification with the fast lithium-ion conductor Li-La-Ti-O, J. Power Sources 364 (2017) 272–279.
[42] W. Pan, W. Peng, H. Guo, J. Wang, Z. Wang, H. Li, K. Shih, Effect of molybdenum substitution on electrochemical performance of Li Li0.2Mn0.54Co0.13Ni0.13 O-2 cathode material, Ceram. Int. 43 (2017) 14836–14841.
[43] X. Yu, Y. Lyu, L. Gu, H. Wu, S.-M. Bak, Y. Zhou, K. Amine, S.N. Ehrlich, H. Li, K.-W. Nam, X.-Q. Yang, Understanding the rate capability of high-energy-density Li-rich layered Li 1.2 Ni 0.15 Co 0.1 Mn 0.55 O 2 cathode materials, Adv. Energy Mater. 4 (2014).
[44] J. Zhao, W. Zhang, A. Huq, S.T. Misture, B. Zhang, S. Guo, L. Wu, Y. Zhu, Z. Chen, K. Amine, F. Pan, J. Bai, F. Wang, In situ probing and synthetic control of cationic ordering in Ni-rich layered oxide cathodes, Adv. Energy Mater. 7 (2017).
[45] M. Hosseini, M. Sarafbidabad, A. Fakhri, Z. NoorMohammadi, S. Tahami, Preparation and characterization of MnS2/chitosan-sodium alginate and calcium alginate nanocomposites for degradation of analgesic drug: photocorrosion, mechanical, antimicrobial and antioxidant properties studies, Int. J. Biol. Macromol. 118 (2018) 1494–1500.
[46] B. Naresh, D. Punnoose, S.S. Rao, A. Subramanian, B.R. Ramesh, H.-J. Kim, Hydrothermal synthesis and pseudocapacitive properties of morphology-tuned nickel sulfide (NiS) nanostructures, New J. Chem. 42 (2018) 2733–2742.
[47] S.S. Zhang, J. Chen, C. Wang, Elemental sulfur as a cathode additive for enhanced rate capability of layered lithium transition metal oxides, J. Electrochem. Soc. 166 (2019) A487–A492.
[48] L. Ban, Y. Yin, W. Zhuang, H. Lu, Z. Wang, S. Lu, Electrochemical performance improvement of Li1.2[Mn0.54Ni0.13Co0.13]O2 cathode material by sulfur incorporation, Electrochim. Acta 180 (2015) 218–226.
[49] G. Assat, A. Iadecola, C. Delacourt, R. Dedryvère, J.-M. Tarascon, Decoupling cationic–anionic redox processes in a model Li-rich cathode via operando X-ray absorption spectroscopy, Chem. Mater. 29 (2017) 9714–9724.
[50] E. Zhao, X. Yu, F. Wang, H. Li, High-capacity lithium-rich cathode oxides with multivalent cationic and anionic redox reactions for lithium ion batteries, Sci. China Chem. 60 (2017) 1483–1493.
[51] X.-D. Zhang, J.-L. Shi, J.-Y. Liang, Y.-X. Yin, Y.-G. Guo, L.-J. Wan, Structurally modulated Li-rich cathode materials through cooperative cation doping and anion hybridization, Sci. China Chem. 60 (2017) 1554–1560.
[52] Y. Cao, X. Qi, K. Hu, Y. Wang, Z. Gan, Y. Li, G. Hu, Z. Peng, K. Du, Conductive polymers encapsulation to enhance electrochemical performance of Ni-rich cathode materials for Li-ion batteries, ACS Appl. Mater. Interfaces 10 (2018) 18270–18280.
[53] D. Mohanty, J. Li, D.P. Abraham, A. Huq, E.A. Payzant, D.L. Wood, C. Daniel, Unraveling the voltage-fade mechanism in high-energy-density lithium-ion batteries: origin of the tetrahedral cations for spinel conversion, Chem. Mater. 26 (2014) 6272–6280.
[54] H.J. Yan, B. Li, N. Jiang, D.G. Xia, First-principles study: the structural stability and sulfur anion redox of Li1-xNiO2-ySy, Acta Physico-Chim. Sin. 33 (2017) 1781–1788.
[55] C. Delmas, Sodium and sodium-ion batteries: 50 Years of research, Adv. Energy Mater. 8 (2018) 1703137.
[56] C. Lin, Y. Tang, J. Song, L. Han, J. Yu, A. Lu, Sr- and Nb-co-doped Li7La3Zr2O12 solid electrolyte with Al2O3 addition towards high ionic conductivity, Appl. Phys. Mater. Sci. Process 124 (2018).

Zhenhe Sun received his B.E. and B.S. degree from the Molecular Science and Engineering department of Nankai University in 2015. He is currently studying for a doctoral degree in Prof. Yongsheng Chen's Group. His research interests include the synthesis and modification of lithium-rich cathode materials and supercapacitors based on carbon materials.

Lingqun Xu received her B.S. degree in Polymer Material and Engineering from the Yanshan University. Now as a postgraduate, her research focuses mainly on improving the cycling performances of lithium sulfur batteries, with an emphasis on the cathode development.

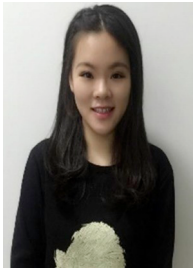

Caiqiao Dong is in the second year of postgraduate courses from the department of chemistry in Nankai University. She majors in Chemical Engineering currently. She received her B.S. degree (2017) from Hebei University of Engineering. Her research interest is the Computational Chemistry.

Dr. Hongtao Zhang obtained his PhD degree at Institute of Chemistry, Chinese Academy of Sciences (ICCAS) in 2012 on the synthesis of organic semiconductor materials for OFET devices. He joined Prof. Yongsheng Chen's group at Nankai University in 2014. His current research interests mainly focus on the synthesis and characterization of efficient energy conversion and storage materials and their application in OPV and batteries.

Mingtao Zhang is a professor from the department of chemistry in Nankai University. He received his B.S. degree and Ph.D. degree from Nankai University in 1993, 2004, respectively. His research interests focus on Molecular Modeling as well as Cheminformatics and Computational Chemistry.

Yanfeng Ma received her B.S. (1994) in Physical Chemistry and Ph.D. (2003) in Physical Chemistry from Nankai university. Since 2003, she has been an Associate Professor of Chemistry at Nankai University. Her research interests focus on controlled synthesis and application of carbon nanomaterials (graphene and carbon nanotubes), carbon-based functional materials, nanocomposites, and nanodevices.

Yiyang Liu graduated from the University of North Carolina at Greensboro with a Ph.D. degree in Nanoscience in 2017 and then joined Zhengzhou University and Nankai University for his postdoctoral studies since 2018. His research interests mainly focus on carbon-based nanomaterials, including carbon nanotubes, graphene, and carbon nanofibers.

Zhongjun Li is a Professor and Dean of the College of Chemistry and Molecular Engineering at Zhengzhou University. He received his Ph.D. from Central South University. His research interests include: 1. Design and synthesis of Photocatalysts for CO2 Reduction; 2. Design and synthesis of photocatalysts for hydrogen production from water under light; 3. Lithium-air batteries\lithium sulfur batteries and other electrochemical energy storage \conversion materials.

Ying Zhou is currently a Ph.D. candidate under the supervision of Prof. Yongsheng Chen at Nankai University. She received her B.E. degree in department of polymeric materials science from Ocean University of China in 2014. Her research focuses on the design and synthesis of electrode materials and their application in lithium ion batteries and lithium metal batteries.

Yu Han is currently a master student at Nankai University under the direction of Prof. Yongsheng Chen. She obtained her B.S. degree from Lanzhou University in 2017. Her main research interests are focused on gel electrolyte and related applications in energy storage.

Prof. Yongsheng Chen graduated from the University of Victoria with a Ph.D. degree in chemistry in 1997 and then joined the University of Kentucky and the University of California at Los Angeles for postdoctoral studies from 1997 to 1999. From 2003, he has been a Chair Professor at Nankai University. His main research interests include: i) carbon-based nanomaterials, including carbon nanotubes and graphene; ii) organic and polymeric functional materials, and iii) energy devices including organic photovoltaics and supercapacitors.